Numerical vibration correlation technique for thin-walled composite beams under compression based on accurate refined finite element

Numerical Vibration Correlation Technique for thin-walled composite beams under compression based on accurate refined finite element

H. Yang[a*], E. Daneshkhah[b†], R. Augello[b‡], X. Xu[c§], E. Carrera[b,d¶]

[a]Nantong University, Sch. Transportat. & Civil Engn., 226019 Nantong, Peoples R China

[b]Mul^2 Group
Department of Mechanical and Aerospace Engineering, Politecnico di Torino
Corso Duca degli Abruzzi 24, 10129 Torino, Italy.

[c]Soochow University, Sch. Rail. Transportat., 215006 Suzhou, Peoples R China.

[d]Department of mechanical engineering, College of engineering,
Prince Mohammad Bin Fahd University P.O. Box 1664. Al Khobar 31952.
Kingdom of Saudi Arabia

Abstract: This paper investigates the virtual vibration correlation technique for the evaluation of the variations of the natural frequencies for highly flexible thin-walled composite beams. In this regard, refined finite element based on the Carrera Unified Formulation (CUF) is developed. Thin-walled composite beams with various cross-sections of box, I-shaped and channel-shaped types, are investigated. Additionally, a comparison of the CUF results with the implemented shell models and the available literature is presented in order to evaluate the accuracy and efficiency of the proposed method. It is indicated that classical beam theories such as Euler–Bernoulli and Timoshenko beam theories failed to have an accurate prediction of the natural frequencies and dynamic response of thin-walled beam structures. Therefore, the necessity of employing higher-order and refined beam theories capable of capturing cross-sectional deformations is highlighted. Furthermore, to fully demonstrate the capabilities of the CUF-1D method with efficient Lagrange expansion, a more complex structural problem of a channel-shaped composite beam with the different numbers of transverse stiffeners is studied, and conclusions about the buckling behavior and variations of natural frequencies are drawn. It is shown that the numerical assessments by the proposed efficient CUF method in this paper correlate well with the shell results which are more computationally expensive.

Keywords: Vibration analysis; Carrera Unified Formulation; Thin-walled composite beam structures; Compressive loads; Vibration Correlation Technique.

---

1 Introduction

Thin-walled composite structures are widely used in different engineering applications such as mechanical components, aerospace, and construction. The use of composite materials provides desir-

*Full Professor
†Ph. D. Student
‡Postdoc. E-mail: riccardo.augello@polito.it
§Full Professor
¶Professor of Aeronautics and Astronautics

able properties of high strength to weight ratio and corrosion resistance. Accurate prediction of mechanical behavior of composite materials has always been a major concern for designers and researchers [1, 2]. Therefore, precise and computationally efficient refined finite element models are required to model these structures. In this regard, one-dimensional beam theories were first developed by Euler [3], Bernoulli [4], Timoshenko [5, 6] and further by Vlasov for thin-walled beams [7, 8].

Free vibration analysis of composite beam structures has been investigated by many researchers [9, 10, 11, 12, 13]. A comprehensive review on the buckling and free vibration of composite beams is presented in the paper by Sayyad and Ghugal [14]. Librescu [15] presented a dynamic solution for thick- and thin-walled composite beams with arbitrary cross-sections. Exact solutions for bending and buckling of cross-ply laminated beams were developed by Khdeir and Reddy [16, 17]. Karama et al. [18] worked on a beam model based on the discrete layer theory for the buckling and free vibration of composite beams. A theoretical model incorporating shear flexibility and state of initial stresses was developed by Cortínez and Piovan [19] for the vibration of thin-walled composite beams. The same authors developed exact analytical solutions for the free vibration analysis of thin-walled composite beams with shear flexibility [20]. Sheikh et al. [21] analyzed the free vibration response of thin-walled composite beams and proposed a one-dimensional modeling technique for the transverse shear deformation and out of plane warping of the beam. The Generalized Beam Theory (GBT) initially introduced by Schardt [22] and further developed by Camotim and Silvestre [23, 24, 25] was efficiently used for the vibration analysis of many thin-walled composite structures.

Many engineering structures are subjected to axial loads in their applications. Hence, an accurate prediction of the vibration response and buckling loads of these structures is of primary importance for the designers and researchers [26, 27, 28]. According to the fact that natural frequencies of the structure are decreased by the axial loads, the vibration Correlation Technique (VCT) [29] is used as a nondestructive method to evaluate the buckling loads of a structure subjected to progressive compression. With the assumption that the vibration and buckling modes are similar, one can extrapolate the critical buckling load as the load that results in the zero natural frequency [30, 31]. Abramovich [32] investigated natural frequencies of Timoshenko beams under compressive loads. Considering the warping effects, Piana et al. analyzed the vibration and buckling of thin-walled beams with symmetric cross-sections [33, 34]. The same authors also compared the numerical and experimental results for a thin-walled non-symmetric cruciform beam under compression [35]. Elkaimbillah et al. [36] developed a one-dimensional finite element model in order to evaluate the forced nonlinear vibration response of thin-walled composite beams. The dynamic stiffness method was used for the free vibration analysis of composite Timoshenko beams under axial loads [37]. Jun et al. [38, 39, 40] used the dynamic stiffness method to evaluate the free vibration response of composite beams subjected to axial loads. Vo and Thai [41] worked on the free vibration response of rectangular composite beams under axial loads by employing shear deformation theory. They also compared the results of triply axial-flexural coupled vibration (axial, bending, and shear components) with uncoupled solutions.

Thin-walled composite beams under axial loads have been further studied in many research papers [42, 43]. Considering the coupling of flexural and torsional modes, many analytical models have been developed to evaluate the buckling and vibration of thin-walled composite box beams [44, 45, 46, 47]. Using the classical lamination theory and accounting for structural couplings from material anisotropy, Vo and Lee [48] worked on a one-dimensional finite element model in order to investigate the free vibration response of thin-walled composite box beams under axial load. The same authors also developed a finite element model with seven degrees of freedom for the vibration and buckling of thin-walled composite beams with I-shaped cross-section [49, 50]. Kim et al. [51] used dynamic stiffness matrix for spatially coupled free vibration analysis of thin-walled composite beams with I-shaped cross-section.

Carrera Unified Formulation (CUF) has been demonstrated to be a reliable and accurate method for solving various structural dynamic problems [52, 53, 54]. According to the CUF, mass and stiffness matrices of the structure are derived in terms of the independent fundamental nuclei. The

framework of CUF has been employed for the vibration analysis of different laminated beam structures. Carrera et al. [55] implemented refined one-dimensional beam theories for the free vibration response of composite beams. Pagani et al. [56] presented refined dynamic stiffness elements for the free vibration analysis of composite beams. Filippi et al. [57] implemented higher-order expansions based on the Chebyshev polynomials for the free vibration analysis of composite beams. By using the CUF, Yang et al. [58] presented exact solutions for free vibration analysis of composite box and sandwich beams. Xu et al. [59] conducted a comprehensive study on the vibration of thin-walled isotropic beams and presented a benchmark for higher-order modes evaluation of these structures. Augello et al. [60] further developed the CUF-based method for the vibration of isotropic beams subjected to axial displacements and compared the results with experimental methods.

Thin-walled composite beam structures under axial loads are focused on in this paper. Advanced refined finite element based on the CUF is implemented for the thin-walled beams with different cross-sections of the box, I-shaped, and channel-shaped. By employing the virtual vibration correlation technique and the framework of CUF, the variations of natural frequencies under axial loads are investigated. A comprehensive comparison of the results with the implemented shell models and the available literature is presented in order to evaluate the accuracy and efficiency of the proposed method. The importance of employing refined finite element models capable of accurate detection of cross-sectional deformations is outlined. In addition, the CUF-1D method with efficient Lagrange expansion is used for a more complex structural problem of a channel-shaped composite beam with the different numbers of transverse stiffeners subjected to axial loads. It is shown that the numerical assessments by the proposed efficient CUF method match well with the shell models, which are significantly more expensive in terms of computational cost.

2 Preliminaries

A rectangular cartesian coordinate system of Fig. 1 is used for the description of an n layers composite beam with the cross-section domain in the $x-z$ plane and the axis along the y direction. In Fig. 1, A_n refers to the cross-section area related to the n^{th} layer.

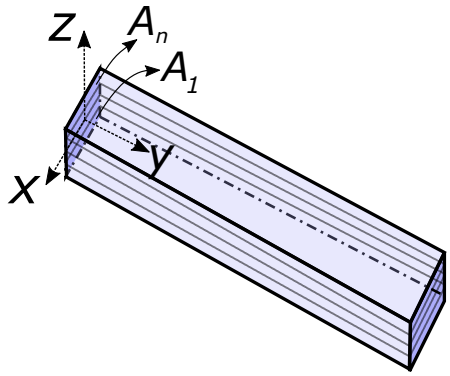

Figure 1: Schematic view of a generic composite beam along the y axis

The displacement, stress, and strain vectors can be defined in the vectorial forms as:

$$\begin{aligned} \boldsymbol{u}(x,y,z) &= \{u_x \;\; u_y \;\; u_z\}^T \\ \boldsymbol{\sigma} &= \{\sigma_{xx} \;\; \sigma_{yy} \;\; \sigma_{zz} \;\; \sigma_{xz} \;\; \sigma_{yz} \;\; \sigma_{xy}\}^T \\ \boldsymbol{\varepsilon} &= \{\varepsilon_{xx} \;\; \varepsilon_{yy} \;\; \varepsilon_{zz} \;\; \varepsilon_{xz} \;\; \varepsilon_{yz} \;\; \varepsilon_{xy}\}^T \end{aligned} \tag{1}$$

If we assume small displacements and rotations, the following geometrical relations for the strains and the displacements can be obtained in the matrix forms:

$$\boldsymbol{\epsilon} = \boldsymbol{D}\,\mathbf{u} \tag{2}$$

Employing the constitutive laws, the stress-strain relationship is formulated as:

$$\boldsymbol{\sigma} = \boldsymbol{C}\,\boldsymbol{\epsilon} \tag{3}$$

For an orthotropic material, the elastic matrix $\boldsymbol{C}$ is reported in [61].

3 CUF and finite element approximation

Based on the CUF, the three-dimensional displacement field of a beam structure in terms of primary unknowns can be expanded as:

$$\boldsymbol{u}(x,y,z;t) = F_\tau(x,z)\,\boldsymbol{u}_\tau(y;t), \qquad \tau = 0,1,\cdots,N, \tag{4}$$

where F_τ is the set of cross-section functions, $\boldsymbol{u}_\tau$ is the generalized displacement vector [62] and τ is the index from 1 to the $N-th$ node. In this paper, the Taylor and Lagrange expansions are adopted for the cross-section functions of the beam structures.

The models based on the Taylor expansion employ polynomial expansion of the kind $x^m z^n$ as cross-section function F_τ, where m and n are positive integers, and the order of model (N) illustrates the structural theory of the beam that is selected as user input. For instance, in the linear case of $N = 1$, the displacement field can be expressed as:

$$\begin{aligned} u_x(x,y,z;t) &= u_{x_1}(y;t) + x u_{x_2}(y;t) + z u_{x_3}(y;t) \\ u_y(x,y,z;t) &= u_{y_1}(y;t) + x u_{y_2}(y;t) + z u_{y_3}(y;t) \\ u_z(x,y,z;t) &= u_{z_1}(y;t) + x u_{z_2}(y;t) + z u_{z_3}(y;t) \end{aligned} \tag{5}$$

The classical beam theories such as Euler–Bernoulli Beam Theory (EBBT) and Timoshenko Beam Theory (TBT) can be obtained as particular cases of linear Taylor expansion [60, 62].
The Lagrange expansion has been used successfully and reliably for several applications such as aerospace and civil industries [63, 64, 65, 66]. The unknown variables are pure displacements for the Lagrange expansions. The Lagrange points can be used where the displacement variables are located. In order to ensure a quadratic interpolation of the variables, in this paper, different numbers of nine-nodes Lagrange polynomials (L9) are adopted for the expansion function over the cross-section. The displacement field evaluated through one L9 polynomial can be expressed as follows:

$$\begin{aligned} u_x(x,y,z;t) &= F_1(x,z)u_{x_1}(y;t) + F_2(x,z)u_{x_2}(y;t) + ... + F_9(x,z)u_{x_9}(y;t) \\ u_y(x,y,z;t) &= F_1(x,z)u_{y_1}(y;t) + F_2(x,z)u_{y_2}(y;t) + ... + F_9(x,z)u_{y_9}(y;t) \\ u_z(x,y,z;t) &= F_1(x,z)u_{z_1}(y;t) + F_2(x,z)u_{z_2}(y;t) + ... + F_9(x,z)u_{z_9}(y;t) \end{aligned} \tag{6}$$

where $u_{x_1}, ..., u_{z_9}$ are the displacements of the points of the cross-sectional elements and $F_1, ..., F_9$ are functions of the cross-sectional coordinates. By using the finite element method for the discretization of the beam structure along the y axis, the generalized displacement vector $\boldsymbol{u}_\tau$ based on the nodal parameters $\boldsymbol{u}_{\tau i}$ and shape functions N_i is defined as follows:

$$\boldsymbol{u}_\tau(y;t) = N_i(y)\,\boldsymbol{u}_{\tau i}(t), \qquad i = 1,2,\ldots,p+1, \tag{7}$$

where N_i represents the i-th shape function and p is related to the order of the shape functions. Note that the shape function can vary along the length of the 1D model of the beam. Interested readers are referred to the book by Bathe [67] for more information about the Lagrange polynomials and shape functions. By using the CUF and finite element approximation, the displacement field is expressed as:

$$\boldsymbol{u}(x,y,z;t) = N_i(y)\,F_\tau(x,z)\,\boldsymbol{u}_{\tau i}(t) \tag{8}$$

According to the Principle of Virtual Displacements (PVD), the equations of motion are as follows:

$$\delta L_{\text{int}} \; + \; \delta L_{\text{ine}} \; = \; \delta L_{ext} \tag{9}$$

where L_{int}, L_{ine}, and L_{ext} represent the strain energy, work of the inertial loadings, and the work of external loadings, respectively. The work of external loadings is here considered as null for the free vibration analysis around trivial equilibrium states; thus, the PVD can be written as:

$$\delta L_{\text{int}} \; + \; \delta L_{\text{ine}} \; = \; 0 \tag{10}$$

By using the CUF as discussed in the previous section, the virtual variations of strain energy can be expressed as:

$$\begin{aligned} \delta L_{\text{int}} &= \int_V \delta \boldsymbol{\varepsilon}^T \boldsymbol{\sigma} dV \\ &= \delta \boldsymbol{u}_{sj}^T \left(\int_V F_s(x,z) N_j(y) \boldsymbol{D}^T \boldsymbol{C} \boldsymbol{D} N_i(y) F_\tau(x,z) dV \right) \boldsymbol{u}_{\tau i} \\ &= \delta \boldsymbol{u}_{sj}^T \boldsymbol{K}^{ij\tau s} \boldsymbol{u}_{\tau i} \end{aligned} \tag{11}$$

and the virtual variations of the inertial work:

$$\begin{aligned} \delta L_{\text{ine}} &= \int_V \delta \boldsymbol{u}^T \rho \ddot{\boldsymbol{u}} dV \\ &= \delta \boldsymbol{u}_{sj}^T \left(\int_V F_s(x,z) N_j(y) \rho N_i(y) F_\tau(x,z) dV \right) \ddot{\boldsymbol{u}}_{\tau i} \\ &= \delta \boldsymbol{u}_{sj}^T \boldsymbol{M}^{ij\tau s} \ddot{\boldsymbol{u}}_{\tau i} \end{aligned} \tag{12}$$

where $\boldsymbol{K}^{ij\tau s}$ and $\boldsymbol{M}^{ij\tau s}$ represent the Fundamental Nuclei (FN) of the stiffness and mass matrices. In the CUF, these FNs are 3×3 matrices for a given i, j pair, and independent of the order of the structure model with a fixed form. Considering all the combinations of the indices i, j, τ, and s, the global matrices of the structure are obtained.

In order to investigate the vibration of structures under axial loads, Eq. (10) should be linearized around non-trivial equilibrium states; as a result:

$$\delta(\delta L_{\text{int}}) = -\delta(\delta L_{\text{ine}}) \tag{13}$$

In the following, $\delta(\delta L_{\text{int}})$ and $\delta(\delta L_{\text{ine}})$ will be assessed by the CUF. The former can be obtained by the linearization of the virtual variation of the internal strain energy as:

$$\delta(\delta L_{\text{int}}) = \int_V \delta(\delta \boldsymbol{\varepsilon}^T \boldsymbol{\sigma}) dV \tag{14}$$

that results in the following equation for the Tangent stiffness matrix [68]:

$$\delta(\delta L_{\text{int}}) = \delta \mathbf{u}_{\tau i}^T \mathbf{K}_T^{ij\tau s} \delta \mathbf{u}_{sj} \tag{15}$$

If we assume small displacements conditions and linear buckling, the tangent stiffness can be approximated as the sum of the linear stiffness ($\boldsymbol{K}_0$) and the geometric stiffness ($\boldsymbol{K}_\sigma$) contribution [30]:

$$\boldsymbol{K}_T \simeq \boldsymbol{K}_0 + \boldsymbol{K}_\sigma \tag{16}$$

If we use the same procedure for the linearization of the virtual variation of the inertia loadings, the following equations are obtained:

$$\begin{aligned}\delta(\delta L_{\text{ine}}) &= \delta\left(\int_V \delta \boldsymbol{u}^T \rho \ddot{\boldsymbol{u}} dV\right) \\ &= \delta\left(\delta \boldsymbol{u}_{sj}^T \boldsymbol{M}^{ij\tau s} \ddot{\boldsymbol{u}}_{\tau i}\right) \\ &= \delta \boldsymbol{u}_{sj}^T \boldsymbol{M}^{ij\tau s} \delta \ddot{\boldsymbol{u}}_{\tau i}\end{aligned} \tag{17}$$

By substituting the virtual variations of strain energy and the inertial work from Eqs. (15) and (17) into Eq. (13), the PVD can be rewritten as:

$$\delta \boldsymbol{u}_{\tau i}^T \boldsymbol{K}_T^{ij\tau s} \delta \boldsymbol{u}_{sj} = -\delta \boldsymbol{u}_{sj}^T \boldsymbol{M}^{ij\tau s} \delta \ddot{\boldsymbol{u}}_{\tau i} \tag{18}$$

By assuming harmonic motion around quasi-static equilibrium states, the eigenvalues problem can be solved as:

$$(-\omega_k^2 \boldsymbol{M} + \boldsymbol{K_T}) \boldsymbol{u}_k = 0 \tag{19}$$

where ω_k are the natural frequencies, and $\boldsymbol{u}_k$ is the k^{th} eigenvector.

4 Numerical results

In this section, numerical results are presented for different thin-walled composite beams under axial loads. The natural frequencies of the beam based on the refined finite element are compared with classical beam theories and the available literature. Furthermore, the variations of natural frequencies for the CUF-1D models based on the Lagrange expansion are compared with the shell models using Abaqus commercial software and the relevant literature. Afterwards, a channel-shaped beam with transverse stiffeners is further investigated.

4.1 Symmetric [90/0/0/90] square beam

The first numerical example is a [90/0/0/90] composite beam with a square cross-section. The beam has the length and width of $l = 6.35$ m and $a = 0.28$ m, respectively, which is simply-supported at both ends. The material properties for this composite beam are shown in Table 1. The values of natural frequencies of the beam are investigated in Table 2 using CUF-1D beam models with Lagrange expansion functions (briefly denoted as CUF-LE in the table) and classical beam theories such as the EBBT and TBT. The obtained values are compared with higher-order beam theories from the literature. Please note that FSDBT, ESDBT, and TSDBT in these tables refer to the first-order, exponential, and trigonometric shear deformation beam theories, respectively. Moreover, the same comparison is presented in Table 3 for the corresponding values of the first three buckling loads. The values of natural frequencies and buckling loads obtained by the CUF and all other higher-order beam theories from the literature show a good agreement. On the other hand, due to the kinematic approximation introduced by the EBBT, the natural frequencies and buckling loads based on the EBBT are higher than the other structural models.

Table 1: Material properties of the 4-layer [90/0/0/90] composite beam [18] with simply-supported edge conditions

E_1 (GPa)	E_2=E_3 (GPa)	G_{12}=G_{13} (GPa)	G_{23} (GPa)	ν_{12}=ν_{13}	ρ ($\frac{kg}{m^3}$)
241.5	18.98	5.18	3.45	0.24	2015

Table 2: Evaluation of the first five natural frequencies of the square composite beam [90/0/0/90] with simply-supported edge conditions based on the CUF-1D models and the literature

Mode number	EBBT	TBT	CUF-LE	FSDBT [38]	Abaqus[18]	TSDBT [39]
Mode 1	15.13	15.00	14.87	14.9	14.95	14.97
Mode 2	60.36	58.41	56.49	58.1	57.6	57.83
Mode 3	135.23	126.10	117.97	124.5	122.8	123.40
Mode 4	238.89	212.78	192.35	208.6	204.2	205.54
Mode 5	370.15	314.06	295.81	304.8	296.6	298.80

Table 3: Evaluation of the first three buckling loads of the square composite beam [90/0/0/90] beam with simply-supported edge conditions based on the CUF-1D models and the literature ($\times 10^6 \frac{\mathrm{N}}{\mathrm{m}}$)

Mode number	EBBT	TBT	CUF-LE	FSDBT [38]	ESDBT[39]	TSDBT [39]
Mode 1	20.71	20.43	20.02	20.44	20.38	20.39
Mode 2	82.70	77.67	73.06	77.07	76.23	76.34
Mode 3	185.44	161.42	150.18	158.23	154.81	155.23

4.2 Unsymmetric [0/θ] square beam

A [0/θ] cantilever square beam is investigated in this section. The length and width of the beam are $l = 1$ m and $b = t = 0.1$ m, respectively. The material properties for this composite beam are as follows [41]:

$$\frac{E_1}{E_2} = 40, \qquad \frac{G_{12}}{E_2} = 0.6, \qquad \frac{G_{23}}{E_2} = 0.5, \qquad \nu_{12} = 0.25 \tag{20}$$

In Table 4, the values of natural frequencies for the composite beams with [0/45] and [0/75] laminations are tabulated. According to this table, the natural frequencies by the classical beam theories such as EBBT and TBT are compared to the ones obtained by the CUF-1D model with Lagrange expansion, Abaqus-3D solid model, and also other higher-order beam theories from reference [41] which consideried coupled solution (axial, bending, and shear components). As can be seen in this table, the natural frequencies obtained by the CUF-LE model correlate well with the corresponding values by the Abaqus-3D solid model and Ref.[41]. However, the ones obtained by the classical theories show some divergences. Therefore, the consideration of higher-order beam theories and refined finite element models for these composite beams is important for accurate analysis of their dynamic bahavior.

Table 4: Evaluation of the first five natural frequencies of the square composite beam [0/θ] with clamped-free edge conditions based on the different structural models and the literature

	[0/45]lamination					[0/75]lamination				
Mode number	EBBT	TBT	CUF-LE	Abaqus	Ref. [41]	EBBT	TBT	CUF-LE	Abaqus	Ref. [41]
Mode 1	4.66	4.59	4.29	4.30	4.32	4.71	4.62	4.18	4.19	4.26
Mode 2	15.57	13.90	12.13	12.96	-	15.76	13.96	11.19	11.27	-
Mode 3	28.83	27.50	20.18	21.57	20.02	42.88	33.65	18.77	20.02	19.73
Mode 4	36.01	34.29	36.62	37.98	-	70.78	35.33	33.64	33.85	-
Mode 5	67.45	45.12	42.89	44.92	44.05	77.96	46.40	42.33	43.66	43.22

To further demonstrate the capabilities of the present CUF-based method for the investigation of the variations of natural frequencies with the axial loads, the previous composite beam with [0/45]

and [0/75] laminations is analyzed in Figs. 2 and 3, respectively. In these figures, the nondimensional axial forces and natural frequencies are considered as follows [41]:

$$\overline{P} = \frac{P\, l^2}{b^3\, t\, E_2}, \qquad \overline{w} = \frac{w\, l^2}{b}\sqrt{\frac{\rho}{E_2}} \tag{21}$$

The natural frequencies are decreased significantly due to the presence of axial loads. The critical buckling load can be considered as the load that results in the zero natural frequency. The results obtained by the CUF-1D approach are in good agreement with the coupled solution from [41] using higher-order beam theories. As correctly highlighted in [41] and also evident from the figures, the reference uncoupled solution is no longer valid for unsymmetrically laminated beams and triply coupled vibration (axial, bending and shear components) should be considered. This is automatically considered by using the presented CUF-1D models with efficient Lagrange expansions.

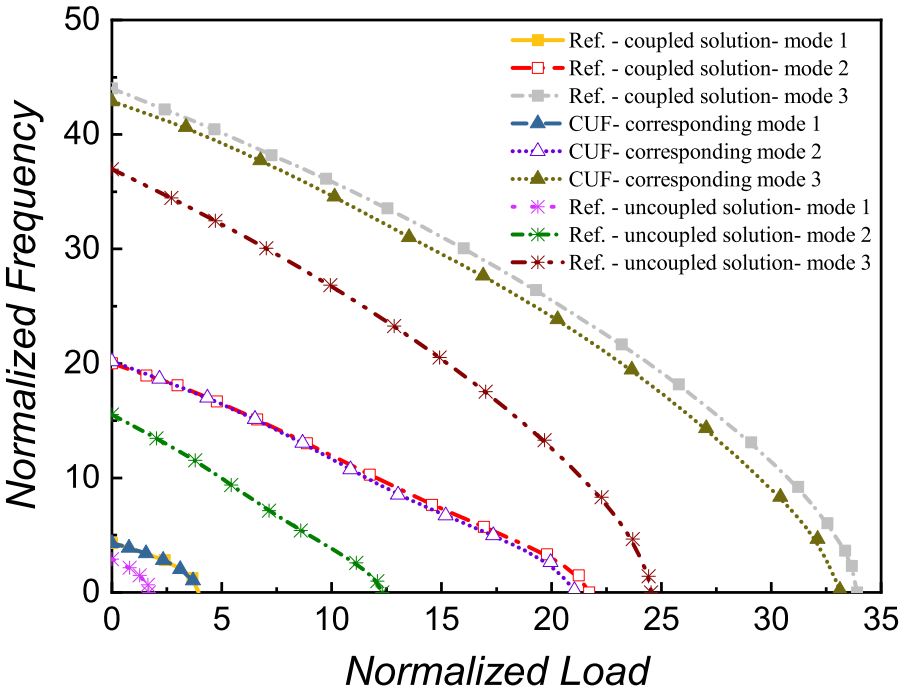

Figure 2: The variations of natural frequencies with the axial loads for the square composite beam with [0/45] lamination based on the CUF-1D model with Lagrange expansion and the available literature [41]

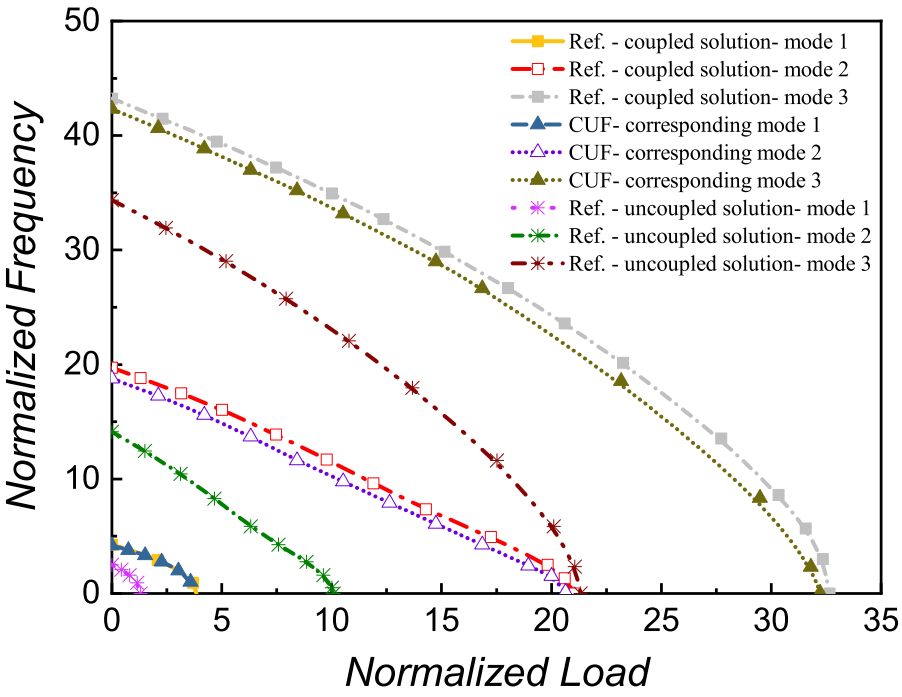

Figure 3: The variations of natural frequencies with the axial loads for the square composite beam with [0/75] lamination based on the CUF-1D model with Lagrange expansion and the available literature [41]

4.3 Thin-walled box beam

In this section, a thin-walled composite box beam with a length of $l = 8$ m and simply-supported edge conditions is studied (See Fig. 4 for the beam geometries). Similar to the previous beam example, Eqs. 21 are used for the normalization of axial loads and natural frequencies. The material properties for this composite beam are [48]:

$$\frac{E_1}{E_2} = 25, \qquad \frac{G_{12}}{E_2} = 0.6, \qquad \nu_{12} = 0.25 \tag{22}$$

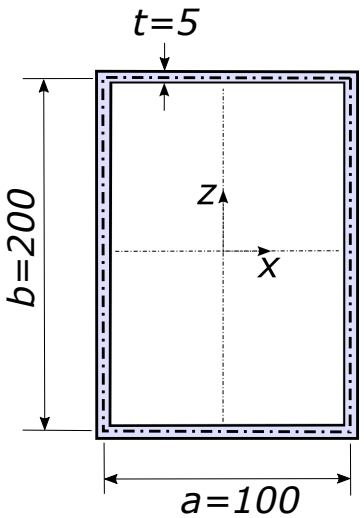

Figure 4: Geometry of thin-walled box beam (dimensions in mm)

The values of natural frequencies based on the classical theories, CUF-1D, Abaqus shell, and Ref. [48] are reported in Table 5 for the composite box beams with [0] and [30/-30] laminations. A good agreement is seen between the results obtained by the CUF-1D, Abaqus shell, and higher-order beam theories of Ref. [48]. Furthermore, in Fig. 6, the vibration modes of this composite beam obtained by the CU-1D models with Lagrange expansion are compared with the ones by Abaqus shell models. Although the CUF-1D models require much less computational effort in comparison with expensive shell ones, the natural frequencies and vibration modes by the two methods match well. Therefore, the present proposed method can be used efficiently for the evaluation of the dynamic response of these structures. For the sake of completeness, the first nine mode shapes of this composite box beam with [0] lamination based on the CUF-1D model with Lagrange expansion are displayed in Table 7.

Table 5: Evaluation of the first six natural frequencies of the composite box beam with simply-supported edge conditions based on the different structural models and the literature

	[0]lamination					[30/-30] lamination in the webs				
Mode number	EBBT	TBT	CUF-LE	Abaqus shell	Ref. [48]	EBBT	TBT	CUF-LE	Abaqus shell	Ref. [48]
Mode 1	10.89	10.82	10.62	10.59	10.88	6.68	6.68	5.21	4.97	6.68
Mode 2	18.39	18.07	17.89	17.87	18.39	15.49	15.29	14.48	14.38	15.49
Mode 3	43.53	42.49	39.61	39.04	45.54	26.71	26.62	20.55	18.44	26.70
Mode 4	73.45	68.75	66.34	66.08	-	60.06	59.61	45.15	40.59	-
Mode 5	-	-	76.11	69.68	-	61.86	58.97	55.00	56.28	-
Mode 6	97.86	92.81	80.76	77.11	-	106.67	105.26	77.71	71.82	-

Table 6: The comparison of vibration mode shapes for the composite box beam with simply-supported edge conditions based on the CUF-1D with Lagrange expansion and Abaqus shell models

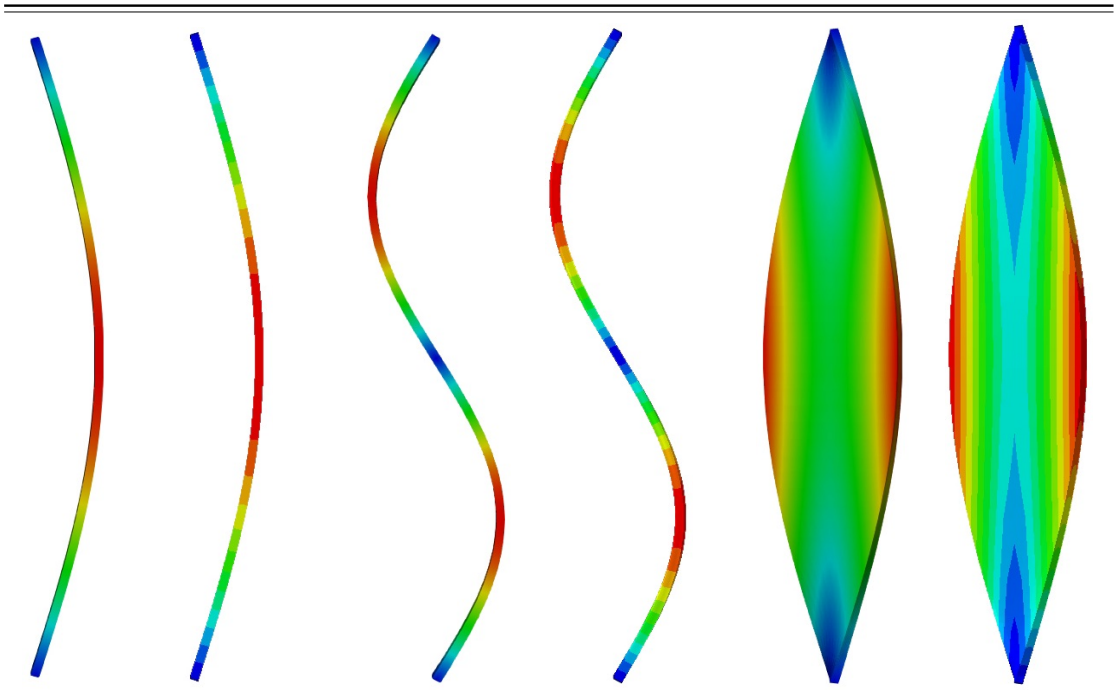

In order to investigate the effects of axial loads on the natural frequencies of thin-walled composite box beams, the results obtained by the CUF-1D models with Lagrange expansion, Abaqus shell

models, and also higher-order beam theories of Ref. [48] are evaluated in the graphs of Fig. 5. It is evident that the CUF-1D results are in good agreement with Abaqus shell ones and the available literature. It should be noted that the graph for the third mode by Ref. [48] using higher-order beam theories shows some discrepancies with the CUF and Abaqus shell results that could be due to the fact the difference between different theories would be more significant in higher-order modes. However, the proposed CUF-1D method remains efficient also in higher-order modes and correlates well with the Abaqus shell results.

Table 7: First nine mode shapes of the composite box beam with simply-supported edge conditions based on the CUF-1D model with Lagrange expansion

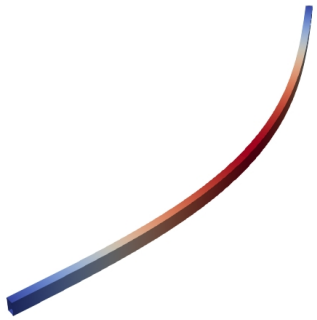	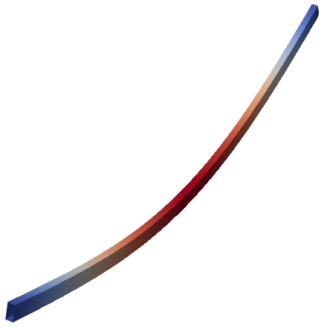	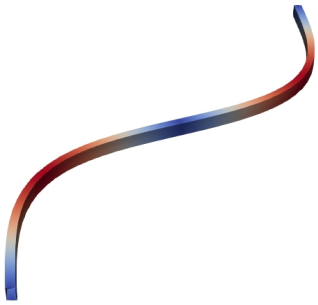
Mode 1	Mode 2	Mode 3
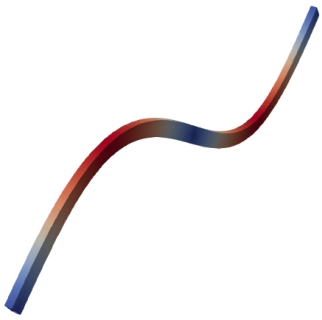	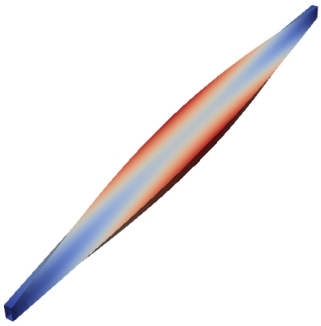	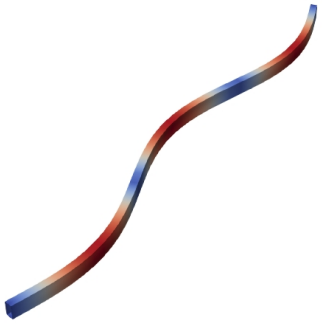
Mode 4	Mode 5	Mode 6
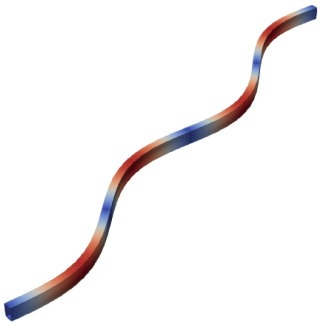	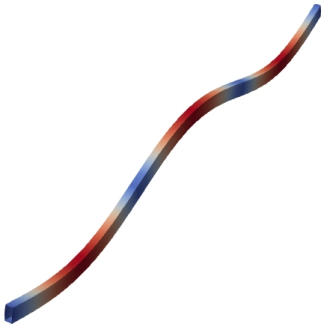	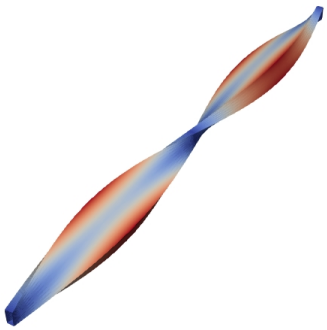
Mode 7	Mode 8	Mode 9

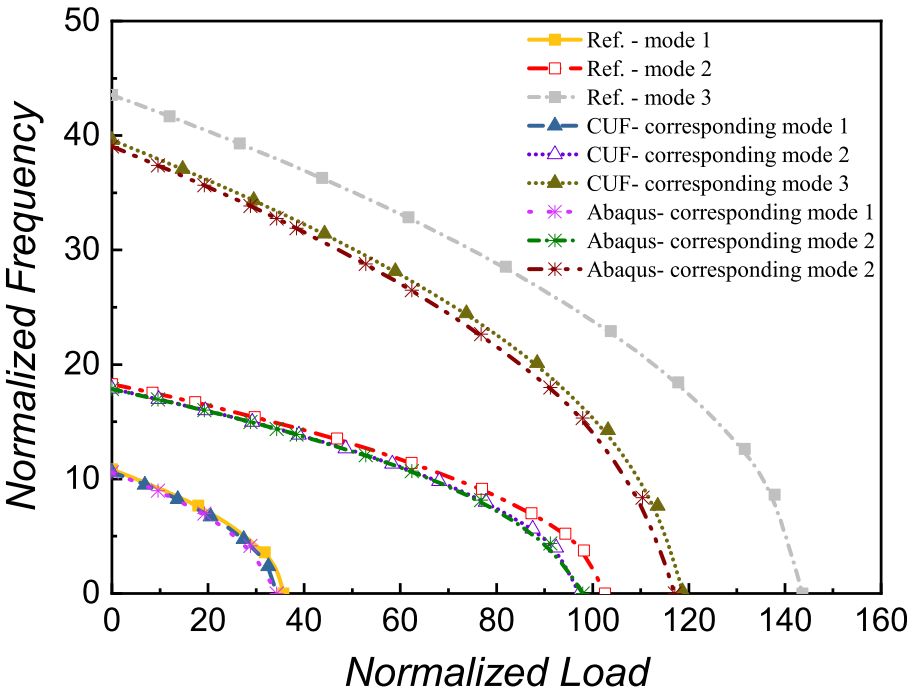

Figure 5: The variations of natural frequencies with the axial loads for the composite box beam based on the CUF-1D model with Lagrange expansion, Abaqus shell, and the available literature [48]

4.4 Thin-walled I-shaped beam

This numerical example focuses on a thin-walled cantilever beam with an I-shaped cross-section. The length of the beam is $l = 1$ m, and the edge conditions are clamped-free. A schematic figure of this beam is depicted in Fig. 6. The material properties for this composite beam are shown in Table 8. The values of natural frequencies for this composite beam with [0] and [60] laminations are tabulated in Table 9 using different structural beam models and also Abaqus shell ones. The values of natural frequencies obtained by the CUF-1D and the higher-order beam theory from the literature [42] show a good agreement with the ones from Abaqus shell models. Due to the kinematic approximation introduced by the EBBT and TBT, the natural frequencies based on these beam theories are higher than the other structural models. Furthermore, some modes with cross-sectional deformations are not captured by these classical beam theories. This highlights the necessity of employing accurate refined finite element methods for the analysis of the dynamic response of these structures. For completeness, the first nine mode shapes of this composite beam with [30] lamination based on the CUF-1D model with Lagrange expansion is shown in Table 10.

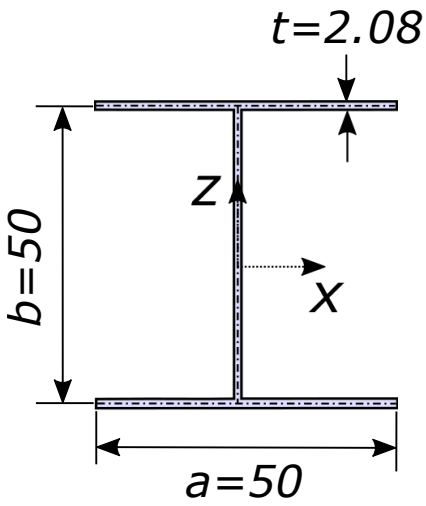

Figure 6: Geometry of thin-walled I-shaped beam (dimensions in mm)

Table 8: Material properties of the thin-walled I-shaped composite beam [42] with clamped-free edge conditions

E_1 (GPa)	E_2 (GPa)	G_{12} (GPa)	ν_{12}	ρ ($\frac{kg}{m^3}$)
53.78	17.93	8.96	0.25	1968.9

Table 9: Evaluation of the first ten natural frequencies of the I-shaped composite beam with clamped-free edge conditions based on the different structural models and the literature

	[0]lamination					[60] lamination				
Mode number	EBBT	TBT	CUF-LE	Abaqus shell	Ref. [42]	EBBT	TBT	CUF-LE	Abaqus shell	Ref. [42]
Mode 1	34.71	34.64	34.61	34.36	34.34	21.04	21.03	20.83	20.68	20.84
Mode 2	-	-	48.45	47.78	-	38.99	38.55	38.30	38.41	-
Mode 3	64.32	63.89	62.98	63.03	-	-	-	40.91	41.21	-
Mode 4	217.11	214.21	211.38	209.75	-	131.61	130.94	129.38	128.52	-
Mode 5	-	-	230.05	228.05	-	-	- 1	62.26	162.57	-
Mode 6	400.39	383.06	348.77	347.48	-	242.71	236.60	228.31	230.35	-
Mode 7	-	-	512.89	505.47	-	367.35	363.03	353.61	353.79	-
Mode 8	-	-	522.66	512.18	-	-	-	387.17	386.31	-
Mode 9	-	-	547.02	536.28	-	-	-	538.53	600.26	-
Mode 10	-	-	570.67	562.32	-	-	-	559.06	660.61	-

Table 10: First nine mode shapes of the I-shaped composite beam with [30] lamination and clamped-free edge conditions based on the CUF-1D model with Lagrange expansion

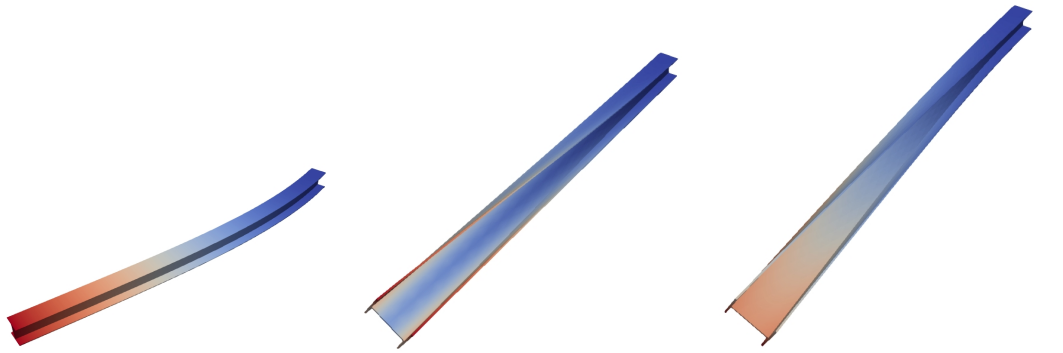		
Mode 1	Mode 2	Mode 3
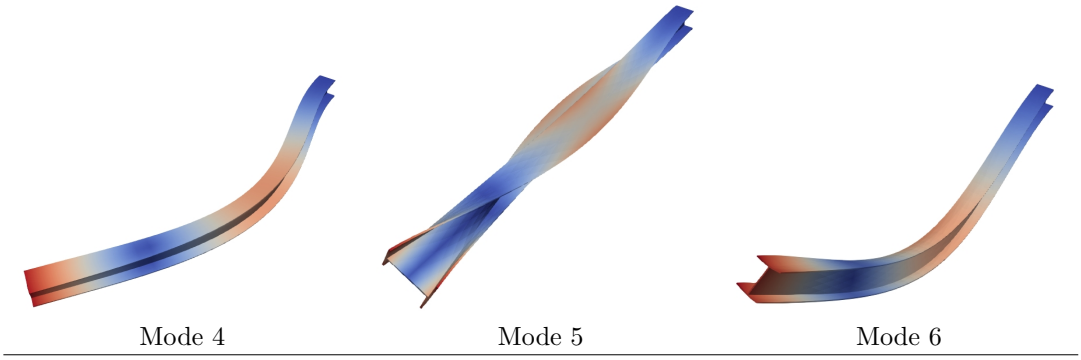		
Mode 4	Mode 5	Mode 6
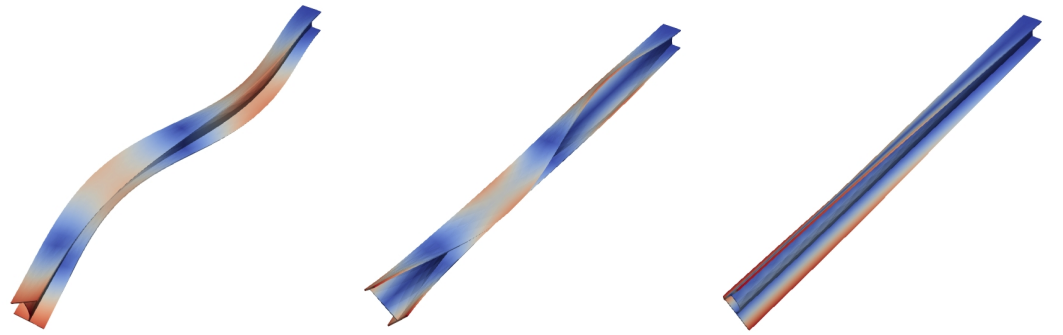		
Mode 7	Mode 8	Mode 9

Similar to the previous numerical examples, the variations of natural frequencies with the axial loads are shown in the graphs of Fig. 7 for this thin-walled beam based on the different structural models. Three different laminations of [0], [30], and [60] are focused here. Due to the fact that for the case of [0] lamination, the fibers are located in the axial direction of the beam, this case shows higher natural frequencies and buckling strength compared to the other investigated laminations. As can be obviously seen in Fig. 7, the results obtained by the proposed cost-effective CUF-1D method match well with the more expensive Abaqus shell models for all the cases.

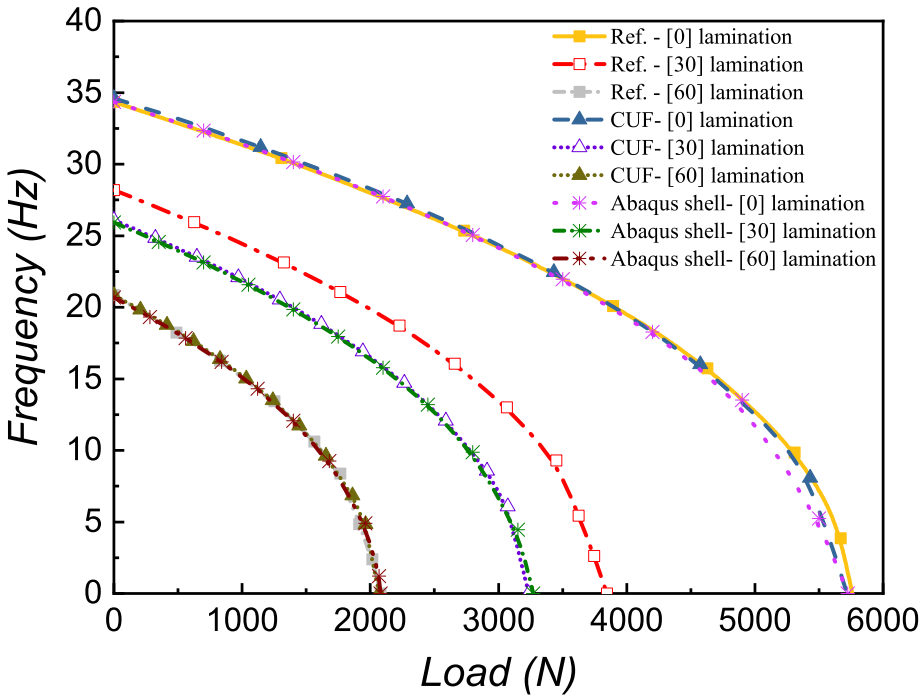

Figure 7: The variations of fundamental frequencies with the axial loads for the I-shaped composite beam based on the CUF-1D model with Lagrange expansion, Abaqus shell model, and the available literature [42]

4.5 Thin-walled Channel-shaped beam

In this section, a thin-walled channel-shaped composite beam with a length of 2 m and clamped-clamped edge conditions is analyzed. A schematic figure of this beam with relevant dimensions is shown in Fig. 8. The material properties for this composite beam are reported in Table 11.

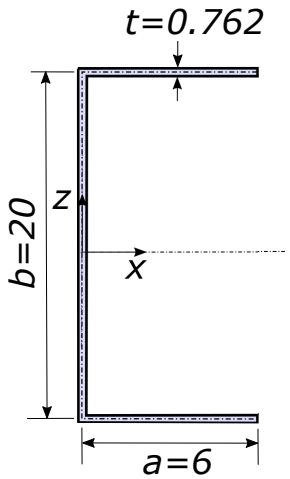

Figure 8: Geometry of thin-walled channel-shaped composite beam (dimensions in mm)

Table 11: Material properties of the channel-shaped composite beam [21] with clamped-clamped edge conditions

E_1 (GPa)	E_2 (GPa)	G_{12}=G_{13} (GPa)	G_{23} (GPa)	ν_{12}	ρ ($\frac{kg}{m^3}$)
141.9	9.78	6.13	4.8	0.42	1445

In tables 12 and 13, the values of natural frequencies based on the CUF-1D, Abaqus shell, Ansys shell from [21], and higher-order beam theories from [21] are compared for the cases of [0], [30], [60], and [90] laminations. A good agreement is seen between the results obtained by the different methods. The first nine mode shapes of this beam based on the CUF-1D model with Lagrange expansion is shown in Table 14.

Table 12: Evaluation of the first ten natural frequencies of the channel-shaped composite beam with clamped-clamped edge conditions based on the different models and the literature

	[0]lamination				[30] lamination			
Mode number	CUF-LE	Abaqus shell	Ansys shell [21]	Higher-order beam theory [21]	CUF-LE	Abaqus shell	Ansys shell [21]	Higher-order beam theory [21]
Mode 1	15.93	15.90	15.90	15.93	6.82	6.75	6.75	8.39
Mode 2	31.11	32.40	34.80	32.69	18.79	18.60	18.61	23.13
Mode 3	43.78	43.70	43.71	43.89	26.30	27.53	27.75	37.27
Mode 4	68.68	71.03	72.93	71.64	36.82	36.46	36.47	45.32
Mode 5	72.27	72.65	75.53	73.10	50.61	50.48	56.31	55.81
Mode 6	85.47	85.34	-	-	60.85	60.30	-	-
Mode 7	116.24	119.31	-	-	63.61	71.72	-	-
Mode 8	140.52	140.34	-	-	90.86	89.95	-	-
Mode 9	175.39	178.83	-	-	93.22	107.39	-	-
Mode 10	193.81	195.43	-	-	103.72	125.12	-	-

Table 13: Evaluation of the first ten natural frequencies of the channel-shaped composite beam with clamped-clamped edge conditions based on the different models and the literature

	[60]lamination				[90] lamination			
Mode number	CUF-LE	Abaqus shell	Ansys shell [21]	Higher-order beam theory [21]	CUF-LE	Abaqus shell	Ansys shell [21]	Higher-order beam theory [21]
Mode 1	4.57	4.53	4.54	4.65	4.20	4.18	4.19	4.18
Mode 2	12.60	12.49	12.50	12.81	11.59	11.53	11.54	11.53
Mode 3	18.47	18.59	18.77	19.37	17.12	17.03	17.12	17.06
Mode 4	24.69	24.48	24.51	25.12	22.71	22.60	22.62	22.62
Mode 5	33.24	36.21	40.48	36.93	31.43	30.99	32.48	31.38
Mode 6	40.81	40.46	-	-	37.54	37.36	-	-
Mode 7	47.86	49.01	-	-	44.61	44.23	-	-
Mode 8	60.97	60.42	-	-	56.08	55.79	-	-
Mode 9	71.06	76.01	-	-	66.81	66.10	-	-
Mode 10	82.84	84.39	-	-	78.32	76.83	-	-

Table 14: First nine mode shapes of the channel-shaped composite beam with clamped-clamped edge conditions based on the CUF-1D model with Lagrange expansion

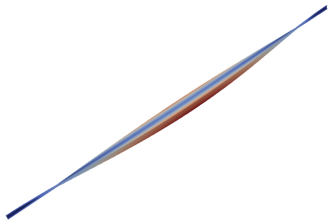	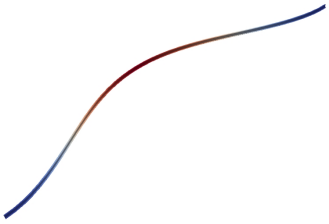	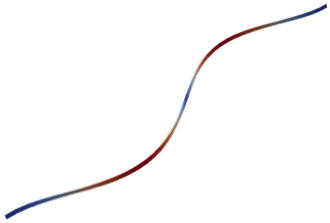
Mode l	Mode 2	Mode 3
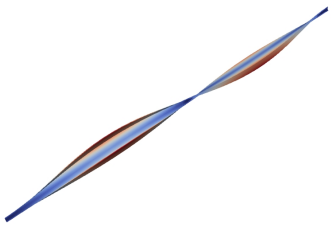	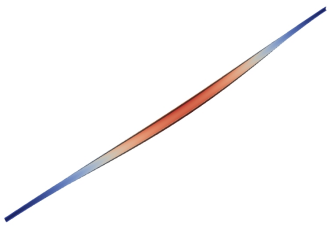	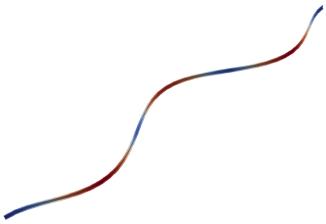
Mode 4	Mode 5	Mode 6
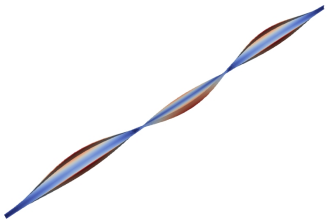	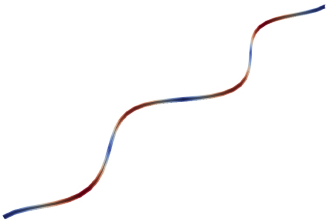	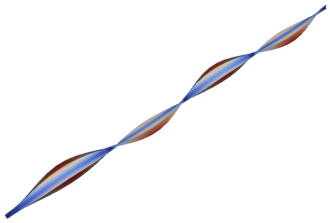
Mode 7	Mode 8	Mode 9

For the evaluation of the effect of axial loads on the variation of natural frequencies for the I-shaped composite beam with [0] lamination, the results obtained by the proposed CUF-1D method with Lagrange expansion and the ones by Abaqus shell models are compared in Fig. 9. The variations of natural frequencies with the axial load for the first five modes of this channel-shaped beam are compared with Abaqus shell models. It can be noticed that the results obtained by the two methods match well for all the first five modes. According to the VCT, and in agreement with the presented results of Fig. 9, the natural frequencies are decreased significantly due to the presence of axial loads. The critical buckling load can be considered as the load that results in the zero natural frequency.

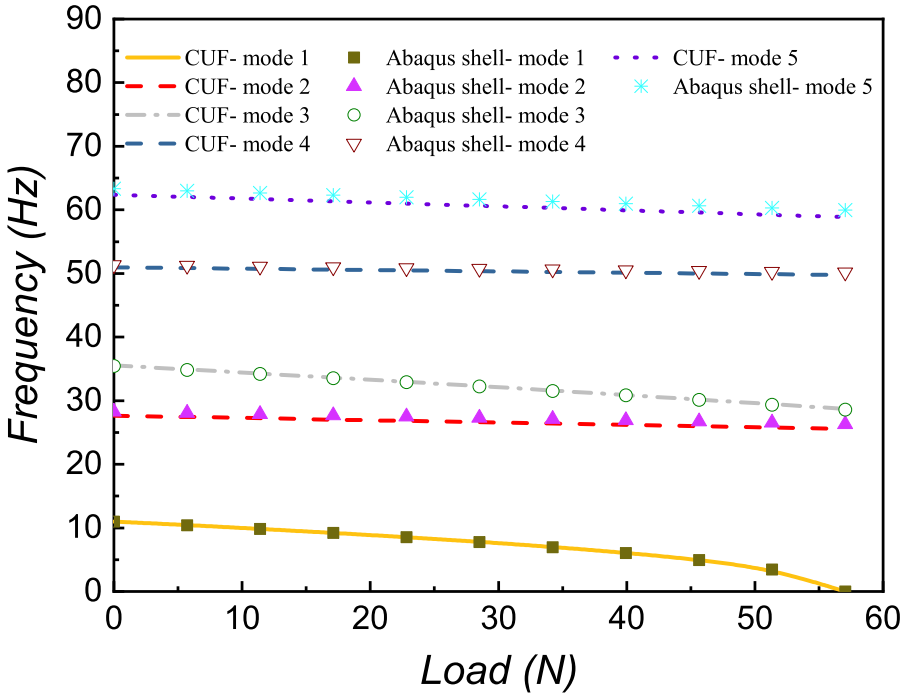

Figure 9: The variations of natural frequencies with the axial loads for the channel-shaped composite beam based on the CUF-1D model with Lagrange expansion and Abaqus shell model

4.6 Channel-shaped beam with transverse stiffeners

In the previous sections, by presenting many numerical assessments and comparisons with the available literature and shell models for different thin-walled composite beams, the reliability and accuracy of the present CUF-based method were shown. In order to fully demonstrate the capabilities of the CUF-1D method with efficient Lagrange expansion, the last numerical assessment corresponds to the channel-shaped beam with transverse stiffeners. The stiffeners are modelled using 1D linear finite elements and Lagrange expansions, as for the cross-section of the beam. For this channel-shaped beam, the dimensions of the web and flanges are all $a = b = 0.6$ m. The beam is simply-supported at both ends, and has the length and thickness of $l = 6$ m and $t = 0.03$ m, respectively. The material properties for this composite beam and the stiffener are reported in Table 15.

Table 15: Material properties of the channel-shaped composite beam [19] with transverse stiffeners and simply-supported edge conditions

E_1 (GPa)	E_2 (GPa)	G_{12}=G_{13} (GPa)	G_{23} (GPa)	ν_{12}=ν_{13}	ν_{23}	ρ ($\frac{kg}{m^3}$)
144	9.65	4.14	3.45	0.3	0.5	1389

The first ten natural frequencies of the channel-shaped composite beam with the different number of transverse stiffeners based on the CUF-1D model with Lagrange expansion are reported in Table 16. Moreover, Table 17 shows the corresponding first nine mode shapes of this beam. It should be noted that due to the presence of transverse stiffeners, the complexity of this beam structure is increased remarkably. Therefore, many analytical models based on the beam theories fail to predict the dynamic response accurately. However, by employing the present CUF-based method with efficient Lagrange expansion, the values of natural frequencies and vibration mode shapes can be assessed carefully.

Table 16: Evaluation of the first ten natural frequencies of the channel-shaped composite beam with different number of transverse stiffeners based on the CUF-1D model with Lagrange expansion

Mode number	No stiffener	One stiffener	Three stiffeners	Five stiffeners
Mode 1	22.42	29.43	28.58	35.52
Mode 2	24.01	30.68	55.00	81.94
Mode 3	30.06	33.01	67.57	96.92
Mode 4	35.63	35.86	69.36	101.67
Mode 5	46.42	58.13	71.29	122.28
Mode 6	50.70	68.67	72.02	143.92
Mode 7	66.19	71.03	78.83	185.75
Mode 8	68.25	72.67	89.01	156.66
Mode 9	71.54	86.66	101.83	166.02
Mode 10	74.57	60.79	129.55	166.51

The final assessments for the investigation of the effects of axial loads on the variations of the first three natural frequencies are shown in Figs. 10 and 11 for the channel-shaped beam with transverse stiffeners and [0] lamination. In these figures, Eqs. 21 are employed for the normalization of axial loads and natural frequencies. The comparison of the beam without stiffener and the beam with one stiffener is shown in Fig. 10. Similarly, the beams with three and five stiffeners are compared in Fig. 11. These figures show how the buckling behavior and natural frequencies of this beam structure are influenced by the number of transverse stiffeners. The maximum natural frequency is seen for the third mode of the case with five stiffeners. Please note that adding the stiffeners changes the mode shapes and natural frequencies of the beam structure completely. Hence, one by one comparison of the modes may not be possible for the different number of stiffeners. For instance, as can be understood from Fig. 10, the maximum natural frequency in the unloaded condition occurs in the third mode of the model with one stiffener. However, its buckling strength is significantly lower than the second mode of the beam without stiffener (See the olive curve with empty circle markers compared to the blue curve with filled triangle markers in Fig. 10). Other examples from Fig. 11 are the second and third modes of the beam with five stiffeners where the former shows the maximum buckling strength; while the latter shows the maximum natural frequency in the unloaded condition.

Table 17: First nine mode shapes of the channel-shaped composite beam with simply-supported edge conditions based on the CUF-1D model with Lagrange expansion

No transverse stiffener	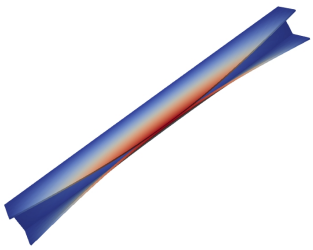 Mode l	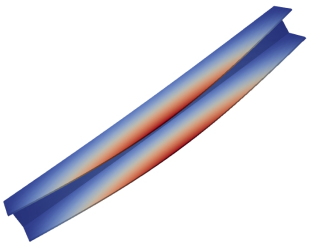 Mode 2	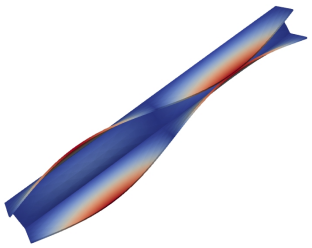 Mode 3
One transverse stiffener	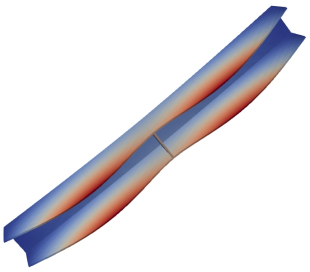 Mode 1	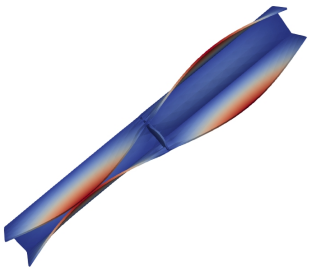 Mode 2	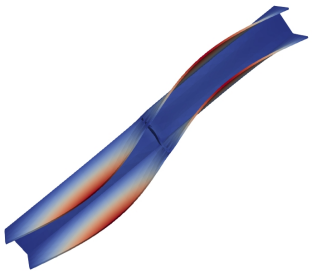 Mode 3
Three transverse stiffeners	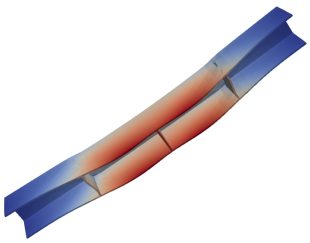 Mode 1	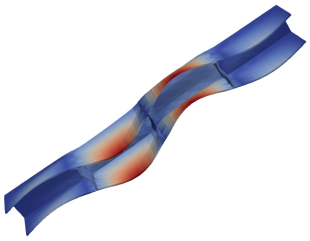 Mode 2	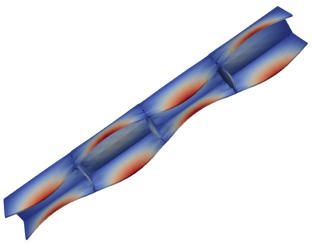 Mode 3
Five transverse stiffeners	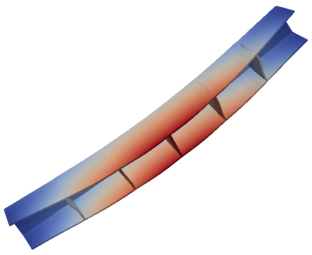 Mode 1	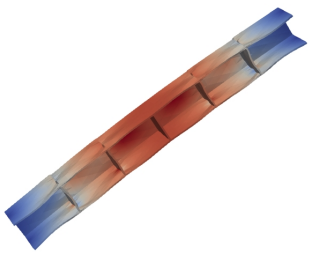 Mode 2	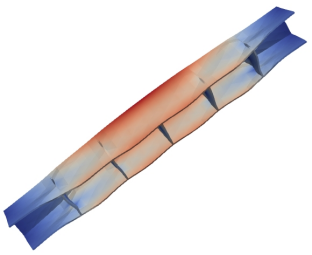 Mode 3

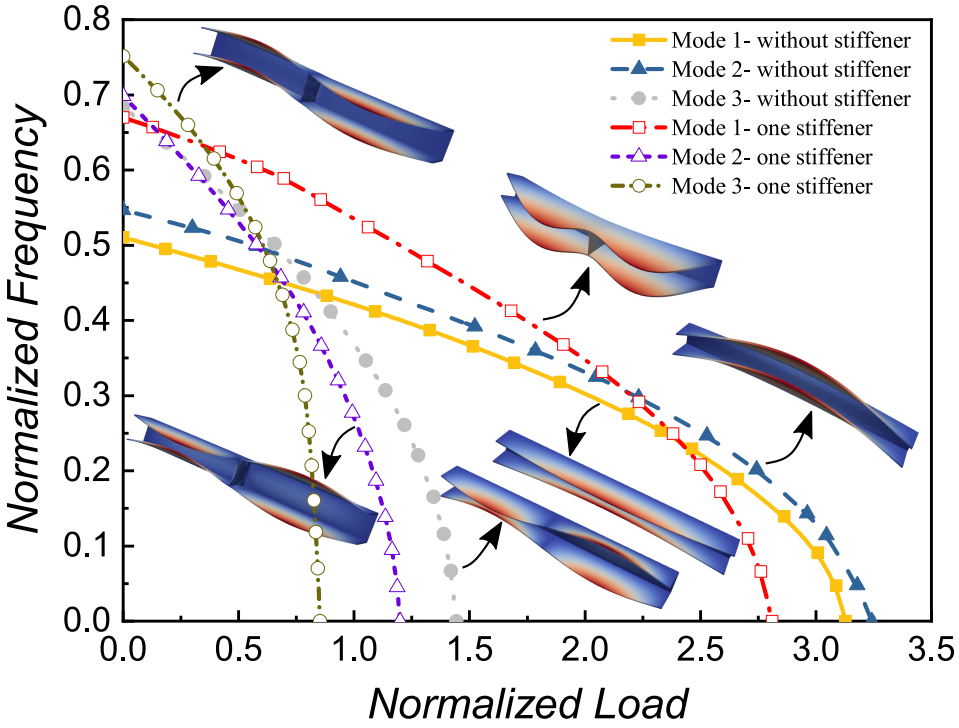

Figure 10: The comparison of natural frequencies variations for the channel-shaped beam without stiffener and with one stiffener

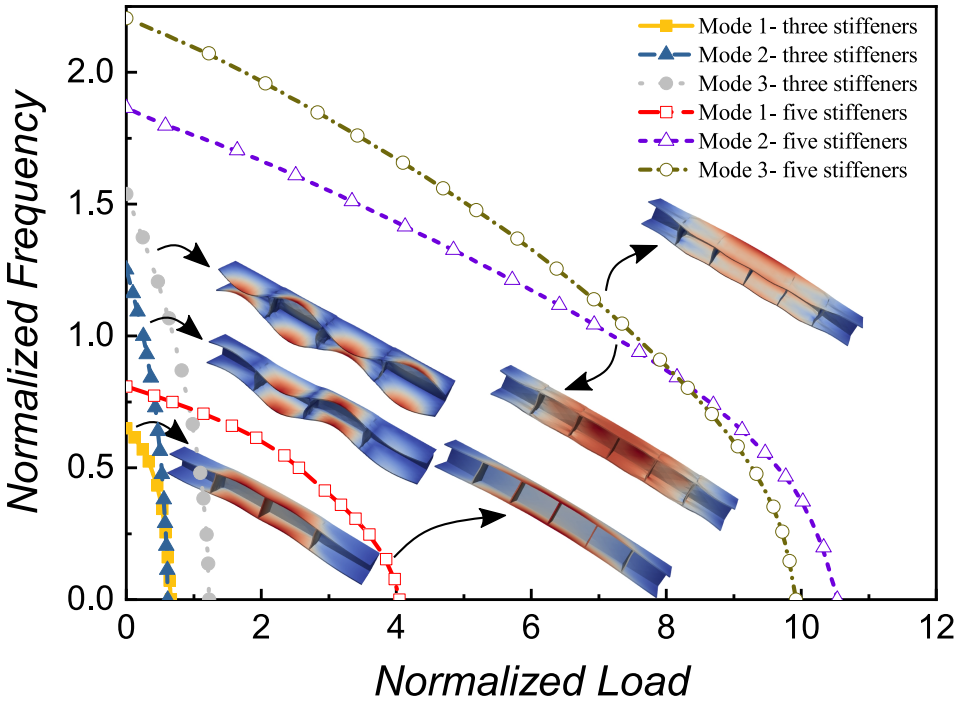

Figure 11: The comparison of natural frequencies variations for the channel-shaped beam with three and five stiffeners

5 Conclusions

In this paper, an accurate refined finite element based on the CUF framework was developed and implemented in order to investigate the vibration response and natural frequencies of thin-walled composite beams under compression. First, composite beams with square cross-sections were studied in order to evaluate the values of natural frequencies and buckling loads of the beam structure. Then different thin-walled beams with box, I-shaped, and channel-shaped cross-sections were analyzed. The natural frequencies and VCT curves were compared with the Abaqus shell results and also the available literature using higher-order beam theories. The results of the proposed CUF-based method were in good agreement with the shell results, which were remarkably more expensive in terms of computational cost. It was shown that many of the vibration modes were missed by the classical beam theories, and they could not predict the natural frequencies and dynamic response of these thin-walled beam structures accurately. Therefore, the necessity of employing higher-order and refined beam theories capable of capturing cross-sectional deformations was highlighted.
The capabilities of the CUF-1D method with efficient Lagrange expansion were shown for a more complex structural problem of a channel-shaped composite beam with different numbers of transverse stiffeners subjected to the compression. The results show that the addition of stiffeners completely changed the mode shapes and natural frequencies of the beam structure. It was observed that some models with higher natural frequencies in the unloaded condition of the VCT graph did not necessarily show high buckling strength. Future extension should focus on the effect of transverse stiffeners nonlinearities on the dynamic response of the beam structures under compression. Moreoever, it is evident how the way the structure is constrained has a direct effect on its structural (static, dynamic and buckling) behaviour. For this reason, a further investigation on the effects of the boundary conditions deserve a dedicated work and is going to be conducted.

References

[1] M.R. Forouzan, M.R. Hosseini A., and E. Daneshkhah. Damage and residual bending strength in glass-polyester molded grating composite panels after low-velocity impact. *Composite Structures*, 227:111290, 2019.

[2] E. Daneshkhah, R.J. Nedoushan, D. Shahgholian, and N. Sina. Cost-effective method of optimization of stacking sequences in the cylindrical composite shells using genetic algorithm. *European Journal of Computational Mechanics*, pages 115–138, 2020.

[3] L. Euler. Additamentum i: De curvas elasticis. *Leonhardi Euleri Opera omnia*, 1(24):231–297, 1911.

[4] D. Bernoulli. De vibrationibus et sono laminarum elasticarum. *Commentarii Academiae Scientiarum Imperialis Petropolitanae*, 13(1741-3):105–20, 1751.

[5] S.P. Timoshenko. Lxvi. on the correction for shear of the differential equation for transverse vibrations of prismatic bars. *The London, Edinburgh, and Dublin Philosophical Magazine and Journal of Science*, 41(245):744–746, 1921.

[6] S.P. Timoshenko. X. on the transverse vibrations of bars of uniform cross-section. *The London, Edinburgh, and Dublin Philosophical Magazine and Journal of Science*, 43(253):125–131, 1922.

[7] V.Z. Vlasov. Thin-walled elastic beams. *PST Catalogue*, 428, 1959.

[8] V.Z. Vlasov. Thin-walled elastic rods. *Fizmatgiz, Moscow*, 1959.

[9] O. Song and L. Librescu. Structural modeling and free vibration analysis of rotating composite thin-walled beams. *Journal of the American Helicopter Society*, 42(4):358–369, 1997.

[10] J.R. Banerjee, H. Su, and C. Jayatunga. A dynamic stiffness element for free vibration analysis of composite beams and its application to aircraft wings. *Computers & Structures*, 86(6):573–579, 2008.

[11] R.A. Jafari-Talookolaei, M.H. Kargarnovin, and M.T. Ahmadian. Free vibration analysis of cross-ply layered composite beams with finite length on elastic foundation. *International Journal of Computational Methods*, 5(01):21–36, 2008.

[12] L.L. Ke, J. Yang, and S. Kitipornchai. Nonlinear free vibration of functionally graded carbon nanotube-reinforced composite beams. *Composite Structures*, 92(3):676–683, 2010.

[13] J. Liu, S. Huang, J. Li, and Y.F. Chen. Vibration serviceability of large-span steel–concrete composite beam with precast hollow core slabs under walking impact. *Engineering*, 2021.

[14] A.S. Sayyad and Y.M. Ghugal. Bending, buckling and free vibration of laminated composite and sandwich beams: A critical review of literature. *Composite Structures*, 171:486–504, 2017.

[15] O. Song and L. Librescu. Free vibration of anisotropic composite thin-walled beams of closed cross-section contour. *Journal of Sound and Vibration*, 167(1):129–147, 1993.

[16] A.A. Khdeir and J.N. Reddy. Buckling of cross-ply laminated beams with arbitrary boundary conditions. *Composite Structures*, 37(1):1–3, 1997.

[17] A.A. Khdeir and J.N. Reddy. An exact solution for the bending of thin and thick cross-ply laminated beams. *Composite Structures*, 37(2):195–203, 1997.

[18] M. Karama, B. Abou Harb, S. Mistou, and S. Caperaa. Bending, buckling and free vibration of laminated composite with a transverse shear stress continuity model. *Composites Part B: Engineering*, 29(3):223–234, 1998.

[19] V.H. Cortínez and M.T. Piovan. Vibration and buckling of composite thin-walled beams with shear deformability. *Journal of Sound and Vibration*, 258(4):701–723, 2002.

[20] M.T. Piovan, C.P. Filipich, and V.H. Cortínez. Exact solutions for coupled free vibrations of tapered shear-flexible thin-walled composite beams. *Journal of Sound and Vibration*, 316(1-5):298–316, 2008.

[21] A.H. Sheikh, A. Asadi, and O.T. Thomsen. Vibration of thin-walled laminated composite beams having open and closed sections. *Composite Structures*, 134:209–215, 2015.

[22] R. Schardt. Generalized beam theory—an adequate method for coupled stability problems. *Thin-walled structures*, 19(2-4):161–180, 1994.

[23] N. Silvestre and D. Camotim. Gbt-based local and global vibration analysis of loaded composite open-section thin-walled members. *International Journal of Structural Stability and Dynamics*, 6(01):1–29, 2006.

[24] N. Silvestre and D. Camotima. Vibration analysis of composite folded-plate members. *International Journal of Vehicle Structures & Systems (IJVSS)*, 1, 2009.

[25] N. Silvestre and D. Camotim. Generalized beam theory to analyze the vibration of open-section thin-walled composite members. *Journal of Engineering Mechanics*, 139(8):992–1009, 2013.

[26] L.N. Virgin and R.H. Plaut. Effect of axial load on forced vibrations of beams. *Journal of Sound and Vibration*, 168(3):395–405, 1993.

[27] L.N. Virgin. *Vibration of axially-loaded structures*. Cambridge University Press, 2007.

[28] X.Y. Li, X.H. Wang, Y.Y. Chen, Y. Tan, and H.J. Cao. Bending, buckling and free vibration of an axially loaded timoshenko beam with transition parameter: Direction of axial force. *International Journal of Mechanical Sciences*, 176:105545, 2020.

[29] J. Singer, J. Arbocz, and T. Weller. *Buckling experiments*. Second Edittion, 2002.

[30] P. H. Cabral, E. Carrera, H.E. dos Santos, P.H. Galeb, A. Pagani, D. Peeters, and A.P. Prado. Experimental and numerical vibration correlation of pre-stressed laminated reinforced panel. *Mechanics of Advanced Materials and Structures*, pages 1–13, 2020.

[31] H. Abramovich. The vibration correlation technique–a reliable nondestructive method to predict buckling loads of thin walled structures. *Thin-Walled Structures*, page 107308, 2020.

[32] H. Abramovich. Natural frequencies of timoshenko beams under compressive axial loads. *Journal of Sound Vibration*, 157(1):183–189, 1992.

[33] G. Piana, A. Carpinteri, E. Lofrano, and G. Ruta. Vibration and buckling of open twbs with local weakening. *Procedia engineering*, 199:242–247, 2017.

[34] G. Piana, E. Lofrano, A. Manuello, G. Ruta, and A. Carpinteri. Compressive buckling for symmetric twb with non-zero warping stiffness. *Engineering Structures*, 135:246–258, 2017.

[35] G. Piana, E. Lofrano, A. Manuello, and G. Ruta. Natural frequencies and buckling of compressed non-symmetric thin-walled beams. *Thin-Walled Structures*, 111:189–196, 2017.

[36] A. Elkaimbillah, B. Braikat, F. Mohri, and N. Damil. A one-dimensional model for computing forced nonlinear vibration of thin-walled composite beams with open variable cross-sections. *Thin-Walled Structures*, page 107211, 2020.

[37] J.R. Banerjee. Free vibration of axially loaded composite timoshenko beams using the dynamic stiffness matrix method. *Computers & structures*, 69(2):197–208, 1998.

[38] L. Jun, H. Hongxing, and S. Rongying. Dynamic stiffness analysis for free vibrations of axially loaded laminated composite beams. *Composite Structures*, 84(1):87–98, 2008.

[39] L. Jun, H. Xiang, and L. Xiaobin. Free vibration analyses of axially loaded laminated composite beams using a unified higher-order shear deformation theory and dynamic stiffness method. *Composite Structures*, 158:308–322, 2016.

[40] L. Jun and H. Hongxing. Free vibration analyses of axially loaded laminated composite beams based on higher-order shear deformation theory. *Meccanica*, 46(6):1299–1317, 2011.

[41] T.P. Vo and H.T. Thai. Free vibration of axially loaded rectangular composite beams using refined shear deformation theory. *Composite Structures*, 94(11):3379–3387, 2012.

[42] Thuc Phuong Vo, Jaehong Lee, and Kihak Lee. On triply coupled vibrations of axially loaded thin-walled composite beams. *Computers & structures*, 88(3-4):144–153, 2010.

[43] A. Asadi and A.H. Sheikh. Buckling of thin-walled laminated composite beams having open and closed sections subjected to axial load and end moment. In *9th Australasian Congress on Applied Mechanics (ACAM9)*, page 70. Engineers Australia, 2017.

[44] T.P. Vo and J. Lee. Free vibration of thin-walled composite box beams. *Composite Structures*, 84(1):11–20, 2008.

[45] T.P. Vo and J. Lee. Flexural–torsional buckling of thin-walled composite box beams. *Thin-walled structures*, 45(9):790–798, 2007.

[46] T.P. Vo and J. Lee. Interaction curves for vibration and buckling of thin-walled composite box beams under axial loads and end moments. *Applied Mathematical Modelling*, 34(10):3142–3157, 2010.

[47] T.P. Vo, J. Lee, and N. Ahn. On sixfold coupled vibrations of thin-walled composite box beams. *Composite structures*, 89(4):524–535, 2009.

[48] T.P. Vo and J. Lee. Free vibration of axially loaded thin-walled composite box beams. *Composite structures*, 90(2):233–241, 2009.

[49] T.P. Vo and J. Lee. Vibration and buckling of thin-walled composite i-beams with arbitrary lay-ups under axial loads and end moments. *Mechanics of Advanced Materials and Structures*, 20(8):652–665, 2013.

[50] T.P. Vo, J. Lee, K. Lee, and N. Ahn. Vibration analysis of thin-walled composite beams with i-shaped cross-sections. *Composite structures*, 93(2):812–820, 2011.

[51] N.I. Kim, D.K. Shin, and Y.S. Park. Dynamic stiffness matrix of thin-walled composite i-beam with symmetric and arbitrary laminations. *Journal of Sound and Vibration*, 318(1-2):364–388, 2008.

[52] S. Brischetto and E. Carrera. Free vibration analysis for layered shells accounting of variable kinematic and thermo-mechanical coupling. *Shock and Vibration*, 19(2):151–169, 2012.

[53] A. Varello and E. Carrera. Free vibration response of thin and thick nonhomogeneous shells by refined one-dimensional analysis. *Journal of Vibration and Acoustics*, 136(6), 2014.

[54] E. Zappino, T. Cavallo, and E. Carrera. Free vibration analysis of reinforced thin-walled plates and shells through various finite element models. *Mechanics of Advanced Materials and Structures*, 23(9):1005–1018, 2016.

[55] E. Carrera, M. Filippi, P.K. Mahato, and A. Pagani. Advanced models for free vibration analysis of laminated beams with compact and thin-walled open/closed sections. *Journal of Composite Materials*, 49(17):2085–2101, 2015.

[56] A. Pagani, E. Carrera, M. Boscolo, and J.R. Banerjee. Refined dynamic stiffness elements applied to free vibration analysis of generally laminated composite beams with arbitrary boundary conditions. *Composite Structures*, 110:305–316, 2014.

[57] M. Filippi, A. Pagani, M. Petrolo, G. Colonna, and E. Carrera. Static and free vibration analysis of laminated beams by refined theory based on chebyshev polynomials. *Composite Structures*, 132:1248–1259, 2015.

[58] Y. Yan, A. Pagani, and E. Carrera. Exact solutions for free vibration analysis of laminated, box and sandwich beams by refined layer-wise theory. *Composite Structures*, 175:28–45, 2017.

[59] X. Xu, E. Carrera, R. Augello, E. Daneshkhah, and H. Yang. Benchmarks for higher-order modes evaluation in the free vibration response of open thin-walled beams due to the cross-sectional deformations. *Thin-Walled Structures*, 166:107965, 2021.

[60] R. Augello, E. Daneshkhah, X. Xu, and E. Carrera. Efficient cuf-based method for the vibrations of thin-walled open cross-section beams under compression. *Journal of Sound and Vibration*, page 116232, 2021.

[61] B. Wu, A. Pagani, M. Filippi, W.Q. Chen, and E. Carrera. Accurate stress fields of post-buckled laminated composite beams accounting for various kinematics. *International Journal of Non-Linear Mechanics*, 111:60–71, 2019.

[62] E. Carrera, M. Cinefra, M. Petrolo, and E. Zappino. *Finite element analysis of structures through unified formulation.* John Wiley & Sons, 2014.

[63] E. Carrera and A. Pagani. Accurate response of wing structures to free vibration, load factors and non-structural masses. *AIAA Journal*, 54(1):227–241, 2016.

[64] A. Pagani, E. Daneshkhah, X. Xu, and E. Carrera. Evaluation of geometrically nonlinear terms in the large-deflection and post-buckling analysis of isotropic rectangular plates. *International Journal of Non-Linear Mechanics*, 121:103461, 2020.

[65] E. Carrera, R. Azzara, E. Daneshkhah, A. Pagani, and B. Wu. Buckling and post-buckling of anisotropic flat panels subjected to axial and shear in-plane loadings accounting for classical and refined structural and nonlinear theories. *International Journal of Non-Linear Mechanics*, 133:103716, 2021.

[66] E. Carrera, A. Pagani, and M. Petrolo. Refined 1D finite elements for the analysis of secondary, primary, and complete civil engineering structures. *Journal of Structural Engineering*, 141:04014123/1–14, 2015.

[67] K.J. Bathe. *Finite Element Procedure.* Prentice Hall, Upper Saddle River, New Jersey, USA, 1996.

[68] E. Carrera, A. Pagani, and R. Augello. Effect of large displacements on the linearized vibration of composite beams. *International Journal of Non-Linear Mechanics*, 120:103390, 2020.